Korean J. Chem. Eng., **29**(7), 959-963 (2012)
DOI: 10.1007/s11814-011-0265-4

Preparation of nanoporous films from self-assembled poly(vinyl chloride-*g*-methyl methacrylate) graft copolymer

Joo Hwan Koh, Su Jin Byun, Won Seok Chi, and Jong Hak Kim†

Department of Chemical and Biomolecular Engineering, Yonsei University,
262, Seongsanno, Seodaemun-gu, Seoul 130-749, Korea
(*Received 15 July 2011 • accepted 11 October 2011*)

Abstract–We report on the preparation of nanoporous films based on an amphiphilic graft copolymer of poly(vinyl chloride-*graft*-methyl methacrylate), i.e., PVC-*g*-PMMA. The PVC-*g*-PMMA graft copolymer was synthesized via atom transfer radical polymerization (ATRP), as confirmed by nuclear magnetic resonance spectroscopy (^{1}H NMR), Fourier transform-infrared (FT-IR) spectroscopy, and gel permeation chromatography (GPC) analysis. The PVC-*g*-PMMA graft copolymer molecularly self-assembled into nanophase domains of PVC main chains and PMMA side chains, as revealed by wide angle X-ray scattering (WAXS) and transmission electron microscopy (TEM). The graft copolymer film prepared from tetrahydrofuran (THF), a good solvent for both chains, had a random microphase-separated morphology. However, when prepared from dimethyl sulfoxide (DMSO), a solvent selectively good for PVC, the film exhibited a micellar morphology consisting of a PMMA core and a PVC corona. Nanoporous films with different pore sizes and shapes were prepared through the selective etching of PMMA chains using a combined process of UV irradiation and acetic acid treatment.

Key words: Graft Copolymer, Nanoporous Film, Morphology, Microscopy, Atom Transfer Radical Polymerization

INTRODUCTION

The self-assembling behavior of block copolymers has been explored considerably during the past decades in the field of nanotechnology due to the unique properties of block copolymers that can control functional materials at the nanoscale level [1-4]. Recently, block copolymer thin films have been used to fabricate porous thin films for nanomaterials [5-8], antireflection films [9], and chemical separation membranes [10-12]. The removal of the minor component in a microphase-separated block copolymer transforms the polymer thin film into an array of nanopores.

Among many block copolymers, poly(styrene-*block*-methyl methacrylate) (PS-*b*-PMMA) has been widely used to create nanoporous materials due to the easy removal of PMMA domains from the thin films [13,14]. PMMA is known to be selectively degraded via chain scission under ultraviolet (UV) or electron beam irradiation [15]. This selective dissolution allows the formation of nanoporous polymer materials with morphology similar to the parent material. However, there have been only a few reports on the preparation of self-assembled nanoporous materials based on graft copolymers [16-18]. This lack of information may be due to the difficulty of controlling the structure of graft copolymers. Graft copolymers are of particular interest because they are more attractive than block copolymers in terms of cost and ease of synthesis.

In this study, we report on the preparation of nanoporous polymer thin films based on an amphiphilic graft copolymer of poly(vinyl chloride-*graft*-methyl methacrylate) (PVC-*g*-PMMA) synthesized via atom transfer radical polymerization (ATRP). Successful synthesis of the graft copolymer was confirmed by nuclear magnetic resonance spectroscopy (^{1}H NMR), Fourier transform-infrared (FT-IR) spectroscopy, and gel permeation chromatography (GPC) analysis. The morphology of the graft copolymer was characterized by wide angle X-ray scattering (WAXS) and transmission electron microscopy (TEM) and was found to be changed depending on polymer/solvent interactions. UV irradiation and subsequent acetic acid treatment led to a selective degradation of the PMMA chains, producing nanoporous PVC films, as confirmed by field-emission scanning electron microscopy (FE-SEM).

†To whom correspondence should be addressed.
E-mail: jonghak@yonsei.ac.kr

EXPERIMENT

1. Materials

Poly(vinyl chloride) (PVC, M_n=55,000 g/mol, M_w=97,000 g/mol), methyl methacrylate (MMA), copper(I) chloride (CuCl, 99%), and 1,1,4,7,10,10-hexamethyltriethylenetetramine (HMTETA, 99%) were purchased from Aldrich and used as received without further purification. Methanol, 1-methy-2-pyrrolidinone (NMP), dimethyl sulfoxide (DMSO), and tetrahydrofuran (THF) were purchased from J. T. Baker. All solvents and chemicals were reagent grade and used as received without further purification.

2. Synthesis of the PVC-*g*-PMMA Graft Copolymer

Three grams of PVC was dissolved in 75 mL NMP in a round flask at 80 °C. After the solution was cooled to room temperature, 9 mL of MMA, 0.24 g of CuCl, and 0.66 mL of HMTETA were added to the solution and the reaction flask was sealed with a rubber septum. The mixture was stirred to produce a homogeneous solution and purged with nitrogen for 30 min. The mixture was placed in a 90 °C oil bath for 5 h. After polymerization, the resultant polymer solution was diluted with THF. After the solution was passed

through a column with activated Al_2O_3 to remove the catalyst, the solution was precipitated into methanol. The polymer was further purified to completely remove unreacted MMA by thrice dissolving the polymer in NMP and precipitating it in methanol. The PVC-*g*-PMMA graft copolymer was obtained and dried in a vacuum oven overnight at room temperature.

3. Preparation of Nanoporous Films

As-synthesized PVC-*g*-PMMA was dissolved in 2 wt% THF or DMSO. The solutions were stirred at 70 °C in an oil bath to ensure homogeneous mixing of the components. Then, the solutions were spin-coated onto a glass substrate at 2,000 rpm for 20 sec and dried completely in a vacuum oven at 120 °C for two days. The PMMA chains in the PVC-*g*-PMMA graft copolymer were selectively etched by UV irradiation (254 nm) for 100 min in a vacuum chamber and subsequently rinsed thoroughly with acetic acid and water.

4. Characterization

^{1}H NMR measurements were performed at 600 MHz on a high-resolution NMR spectrometer (AVANCE 600 MHz FT-NMR, Bruker, Germany). FT-IR spectra of the samples were collected using an Excalibur Series FT-IR (DIGLAB) instrument in the frequency range of 4,000-600 cm^{-1} using the ATR facility. XRD measurements were conducted on a Rigaku RINT2000 wide-angle goniometer with a Cu cathode operated at 40 kV and 300 mA. TEM images were obtained with a JEOL JEM 1010 microscope operating at 300 kV. For the TEM measurements, the polymers were dissolved in a solvent and then a drop of each solution was placed onto a standard copper grid. The morphologies of the nanoporous films were observed by using FE-SEM (SUPRA 55VP, Carl Zeiss, Germany).

RESULTS AND DISCUSSION

Scheme 1 illustrates the one-step reaction used for the synthesis of the PVC-*g*-PMMA graft copolymer via ATRP. The "grafting-from" approach via the ATRP technique has been established as an efficient polymerization method for the synthesis of well-defined graft copolymers due to the controlled chain growth and living nature of polymerization [16-20]. In this study, the PMMA side chains were grafted from the PVC backbones through direct initiation of the chlorine atoms in vinyl chloride units [19]. The chemical dissimilarity between the hydrophilic PMMA and hydrophobic PVC segments was sufficient to produce a microphase-separated structure of the graft copolymer due to its amphiphilic properties.

The successful graft copolymerization of PMMA side chains from PVC main chains via ATRP was confirmed by ^{1}H NMR, FT-IR, and GPC analysis. The ^{1}H NMR spectrum for the PVC-*g*-PMMA graft copolymer synthesized with a wt. ratio of PVC : MMA=1 : 3

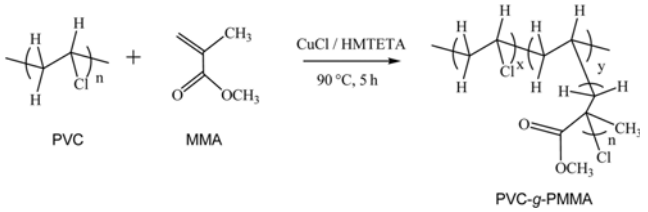

Scheme 1. Synthesis of the PVC-*g*-PMMA graft copolymer via ATRP.

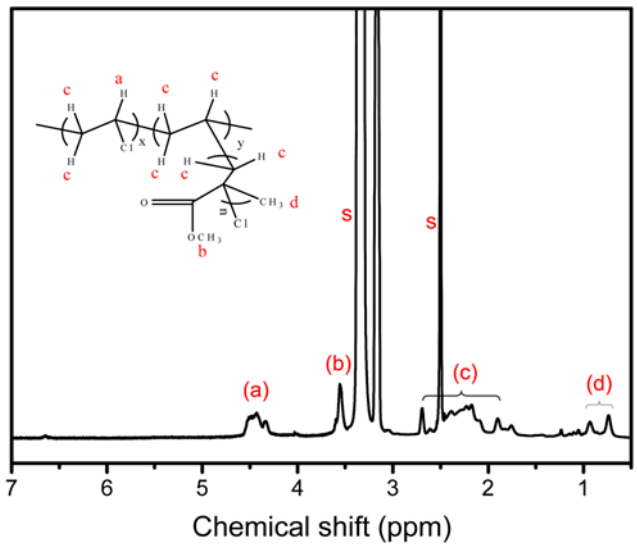

Fig. 1. ^{1}H NMR spectrum for the PVC-*g*-PMMA graft copolymer.

is presented in Fig. 1. The strong peaks at 3.4 and 2.5 ppm are due to water and DMSO, respectively. The peak at around 4.5 ppm is attributed to the CHCl of PVC [19]. Grafting of PMMA from PVC backbones produced an additional peak at 3.5 ppm corresponding to the methoxy group (-OCH_3) in the MMA unit [21], indicating successful grafting via ATRP. The amount of grafted PMMA was determined from the integral ratio of the signals originating from the PMMA at 3.5 ppm and the PVC at 4.5 ppm. Therefore, the actual proportion of grafted PMMA in the PVC-*g*-PMMA copolymer was calculated to be 25 wt%.

The FT-IR spectra in Fig. 2 show the characterization of graft copolymerization of PMMA brushes from PVC main chains via ATRP. Upon graft copolymerization of PMMA from PVC backbones, strong absorption bands at 1,726 (C=O stretching), 1,192, and 1,147 cm^{-1} (C-O stretching) appeared. These peaks shifted from peaks at 1,720, 1,195, and 1,156 cm^{-1} of neat MMA because the bond strength of the C=O and -OCH_3 changed after graft copoly-

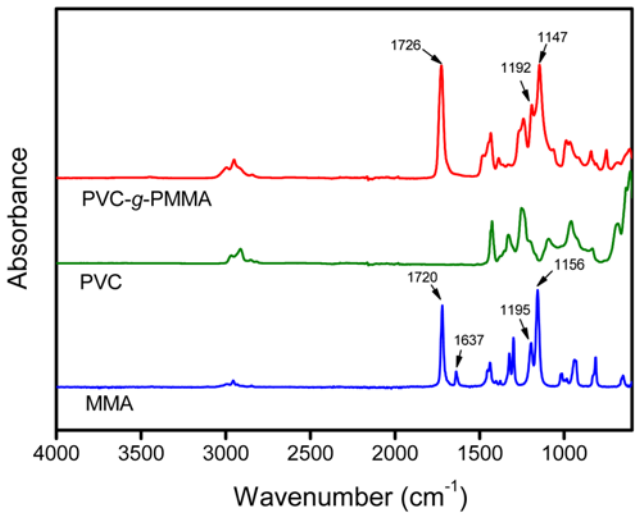

Fig. 2. FT-IR spectra of MMA, PVC, and the PVC-*g*-PMMA graft copolymer.

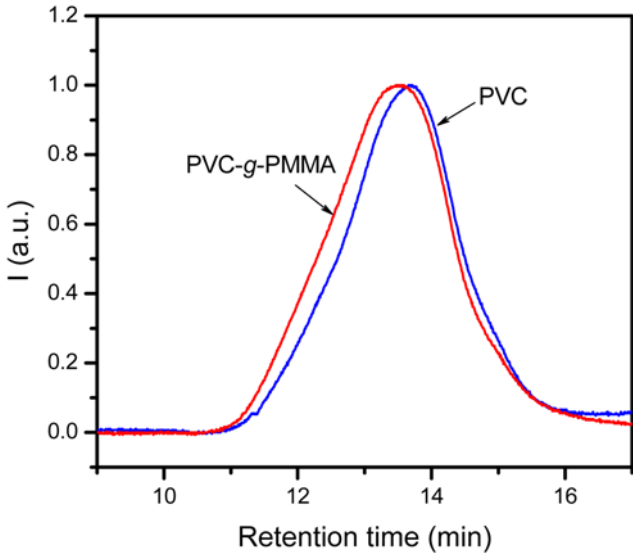

Fig. 3. GPC traces of pristine PVC and the PVC-*g*-PMMA graft copolymer.

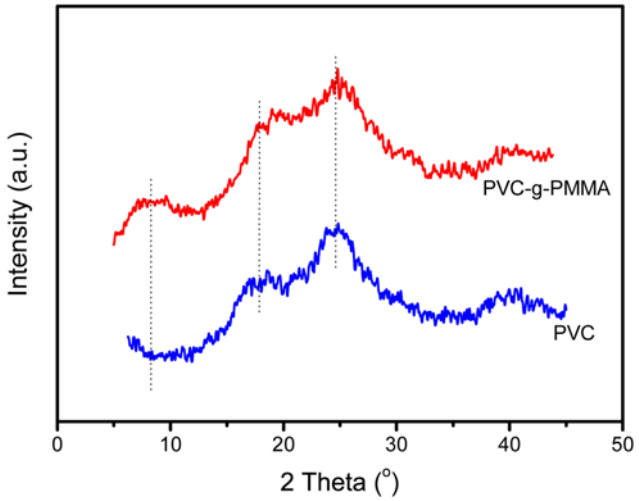

Fig. 4. XRD patterns of pristine PVC and the PVC-*g*-PMMA graft copolymer.

merization through specific interactions, such as hydrogen bonding [22]. In addition, the C=C stretching bond of neat MMA at 1,637 cm^{-1} completely disappeared after the graft copolymerization, confirming the successful synthesis of the PVC-*g*-PMMA graft copolymer.

Fig. 3 shows the GPC traces for the pristine PVC and PVC-*g*-PMMA graft copolymer. The grafting of PMMA from PVC main chains resulted in an upward shift of the distributions in molecular weight relative to the PVC homopolymer (6.6×10^4 to 8.2×10^4 g/mol) and the increase in the polydispersity index (PDI) from 1.8 to 2.2. The molecular weight distribution for PVC-*g*-PMMA graft copolymer was unimodal, indicating no homopolymer contamination or coupling reactions [20]. This result also supports the grafting of PMMA side chains from the PVC backbone via ATRP.

WAXS patterns of pristine PVC and PVC-*g*-PMMA graft copolymer were measured in the range of 5° to 45° to characterize the molecular structure of the graft copolymer. Pristine PVC is an amorphous polymer that exhibits some weak peaks centered at diffraction angles of 18.1°, 24.5°, and 40.0° [23]. The molecular structure and physical network of the polymer were changed upon the grafting of PMMA from the PVC main chains. An additional broad halo appeared in the WAXS pattern at a lower angle of 8.5°, which is attributable to the interchain d-spacing of PMMA pendant side chains [24,25]. However, the main amorphous halos in the PVC backbone were almost unchanged after graft copolymerization, indicating an unperturbed, microphase-separated structure of PVC main chains and PMMA side chains.

TEM showed that the microphase-separated morphology of the PVC-*g*-PMMA graft copolymer differed depending on the casting solvent used, as shown in Fig. 5. Figs. 5(a) and (b) show the TEM images of PVC-*g*-PMMA graft copolymers prepared from THF and DMSO solutions, respectively. These two solvents were chosen for this study because THF is a good solvent for both PVC and PMMA chains, whereas DMSO is a good solvent for the PVC chain

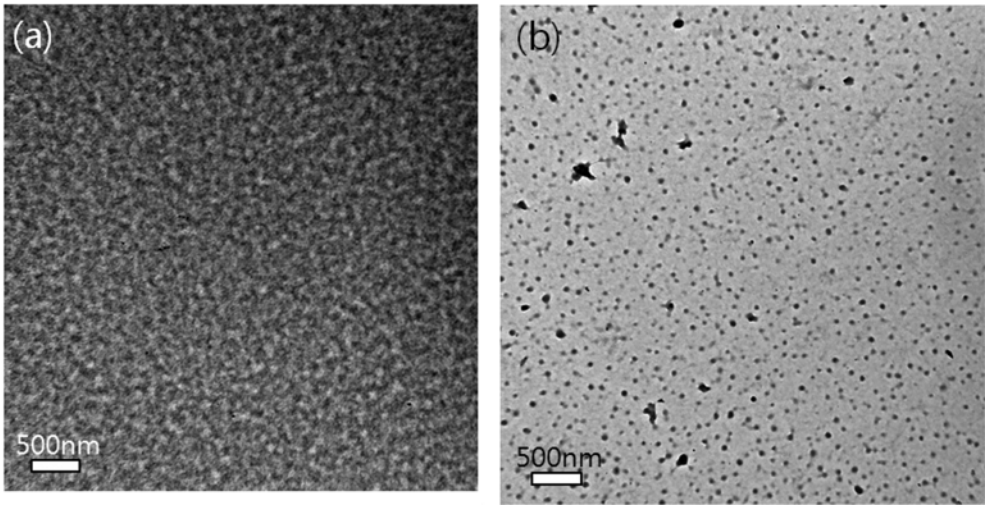

Fig. 5. EF-TEM images of PVC-*g*-PMMA films cast from (a) THF and (b) DMSO.

Table 1. Solubility parameter (δ) of polymers and solvents [26-29]

	PMMA	THF	PVC	DMSO
Solubility parameter ($(J/cm^3)^{1/2}$)	19.0	19.5	22.1	24.5

only. The interaction between polymer and solvent can be estimated based on solubility parameter. The tendency toward solubility is maximized when the solubility parameters of the polymer and solvent are closely matched. The solubility parameters in Table 1 clearly demonstrate that THF is a neutral solvent, whereas DMSO is a preferential solvent for PVC [26-28]. Since THF is a good solvent for both PVC and PMMA, both chains exhibited a stretched conformation, leading to random microphase-separated morphology (Fig. 5(a)), which is commonly observed in a graft copolymer [16-20]. The dark regions in Fig. 5(a) represent the hydrophilic domains of the PMMA side chains, whereas lighter regions, indicating a higher electron density, represent the PVC [16-18]. When films were prepared from DMSO solution, an ordered micellar morphology was observed, as shown in Figure 5b. Since DMSO is a good solvent for PVC only, the interfacial energy between the PVC chains and DMSO was increased, leading to increased stretching of the PVC chains and reduced swelling of the PMMA chains. Thus, the PMMA chains were aggregated to form a cubic-like core of micelles, and the PVC chains formed a corona outside the core. The average core size of the graft copolymer micelles was estimated to be approximately 40 nm.

Fig. 6 shows the FE-SEM images of the PVC-*g*-PMMA films after the selective removal of PMMA chains by UV irradiation and acetic acid treatment. This selective dissolution produced nanoporous PVC films with different structures, depending upon the initial morphology of the graft copolymer prepared from THF or DMSO solutions. When THF was used as a casting solvent, a large interconnected, worm-like nanoporous structure with a length of 50-200 nm and a width of 40-50 nm was observed (Fig. 6(a)). The structure of this nanoporous film was similar to the microphase-separated morphology of the PVC-*g*-PMMA graft copolymer shown in Fig. 5(a). In contrast, the porous film prepared from DMSO (Fig. 6(b)) had a small, spherical, porous structure, which is consistent with the spatial distribution pattern shown in Fig. 5(b). The average pore diameter (~25 nm) in Fig. 6(a) was slightly smaller than that of the micelle core in Fig. 5(b) (~40 nm). This difference may

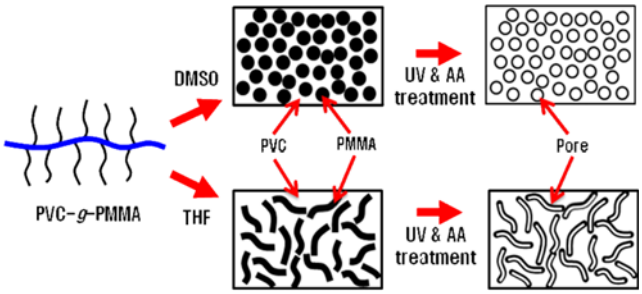

Scheme 2. Schematic process for the formation of nanoporous PVC films.

be due to shrinkage of the nanoporous PVC films after the selective removal of PMMA chains. A schematic illustrating the synthesis of a nanoporous PVC film is shown in Scheme 2.

CONCLUSIONS

This work demonstrated a simple method for fabricating a nanoporous polymer film based on PVC-*g*-PMMA graft copolymers. PVC-*g*-PMMA graft copolymers were synthesized via an ATRP process using a PVC backbone as a macroinitiator, as confirmed by ^{1}H NMR, FT-IR, and GPC analysis. Upon grafting, the molecular weight of the polymer increased from 6.6×10^4 to 8.2×10^4 g/mol and the PDI value increased from 1.8 to 2.2. WAXS patterns revealed that the main amorphous halos in the PVC backbone were almost unchanged, but an additional weak halo appeared at 8.5° due to the interchain d-spacing of the PMMA side chains, indicating a microphase-separated structure. The morphologies of the PVC-*g*-PMMA graft copolymers were strongly dependent on polymer/solvent interactions. The PVC-*g*-PMMA film prepared from THF, a good solvent for both chains, exhibited random microphase-separated morphology. However, the film prepared from DMSO, a solvent selective for PVC, showed a micellar morphology consisting of a PMMA core and a PVC corona. When the films were irradiated by UV light and rinsed with acetic acid, nanoporous PVC films were fabricated by the selective dissolution of the PMMA domain. Removal of the PMMA domain created versatile pore structures over the entire film. The structures of nanoporous PVC films were consistent with the morphology of the parent PVC-*g*-PMMA graft copolymer.

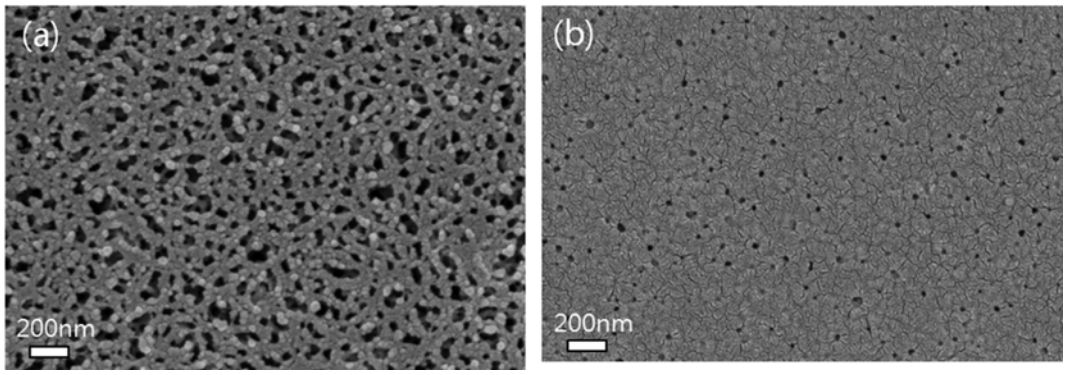

Fig. 6. FE-SEM images of nanoporous PVC films cast from (a) THF and (b) DMSO after removal of PMMA chains.

ACKNOWLEDGEMENTS

This work was supported by the Ministry of Knowledge Economy (MKE) through the Human Resources Development program of the Korea Institute of Energy Technology Evaluation and Planning (KETEP) (20104010100500), and Korea Institute for Advancement in Technology (KIAT) through the Workforce Development Program in Strategic Technology. This work was also supported by a National Research Foundation (NRF) grant funded by the Korean government (MEST) through the Korea Center for Artificial Photosynthesis (KCAP) at Sogang University (NRF-2009-C1AAA001-2009-0093879).

REFERENCES

1. S. I. Stupp, *Curr. Opin. Colloid Interface Sci*., **3**, 20 (1998).
2. C. Park, J. Yoon and E. L. Thomas, *Polymer*, **44**, 6725 (2003).
3. S. J. Jeong, G. Xia, B. H. Kim, D. O. Shin, S. H. Kwon, S. W. Kang and S. O. Kim, *Adv. Mater*., **20**, 1898 (2008).
4. S. H. Park, D. O. Shin, B. H. Kim, D. K. Yoon, K. Kim, S. Y. Lee, S. H. Oh, S. W. Choi, S. C. Jeon and S. O. Kim, *Soft Matter*, **6**, 120 (2010).
5. B. Nandan, B. K. Kuila and M. Stamm, *Eur. Polym. J*., **47**, 584 (2011).
6. X. Li, S. Zhao, S. Zhang, D. H. Kim and W. Knoll, *Langmuir*, **23**, 6883 (2007).
7. C. Wang, D. Wang, X. Hu and G. Wang, *J. Colloid Interface Sci*., **354**, 219 (2011).
8. D. Scalaronea, J. Tataa, F. Calderaa, M. Lazzarib and O. Chiantore, *Mater. Chem. Phys*., **128**, 166 (2011).
9. W. Joo, M. S. Park and J. K. Kim, *Langmuir*, **22**, 7960 (2006).
10. S. Y. Yang, I. Ryu, H. Y. Kim, J. K. Kim, S. K. Jang and T. P. Russell, *Adv. Mater*., **18**, 709 (2006).
11. H. Uehara, M. Kakiage, M. Sekiya, D. Sakuma, T. Yamonobe, N. Takano, A. Barraud, E. Meurville and P. Ryser, *ACS Nano*, **3**, 924 (2009).
12. Y. Li and T. Ito, *Anal. Chem*., **81**, 851 (2009).
13. S. Ibrahim and T. Ito, *Langmuir*, **26**, 2119 (2010).
14. T. Xu, J. Stevens, J. A. Villa, J. T. Goldbach, K. W. Guarini, C. T. Black, C. J. Hawker and T. P. Russell, *Adv. Func. Mater*., **13**, 698 (2003).
15. T. Thurn-Albrecht, R. Steiner, J. DeRouchey, C. M. Stafford, E. Huang, M. Bal, M. Tuominen, C. J. Hawker and T. P. Russell, *Adv. Mater*., **12**, 787 (2000).
16. S. H. Ahn, J. H. Koh, J. A. Seo and J. H. Kim, *Chem. Commun*., **46**, 1935 (2010).
17. S. H. Ahn, H. Jeon, K. J. Son, H. Ahn, W. G. Koh, D. Y. Ryu and J. H. Kim, *J. Mater. Chem*., **21**, 1772 (2011).
18. J. H. Koh, J. A. Seo, J. K. Koh and J. H. Kim, *Nanotechnology*, **21**, 355604 (2010).
19. G. Chen, X. Zhu, Z. Cheng and J. Lu, *J. Appl. Polym. Sci*., **96**, 183 (2005).
20. M. Zhang and T. P. Russell, *Macromolecules*, **39**, 3531 (2006).
21. H. Durmaz, A. Dag, O. Altintas, T. Erdogan, G. Hizal and U. Tunca, *Macromolecules*, **40**, 191 (2007).
22. M. Guvendiren, P. A. Heiney and S. Yang, *Macromolecules*, **42**, 6606 (2009).
23. S. H. Ahn, J. A. Seo, J. H. Kim, Y. Ko and S. U Hong, *J. Membr. Sci*., **345**, 128 (2009).
24. M. Aguilar-Vega and D. R. Paul, *J. Polym. Sci., B*, **31**, 1577 (1993).
25. S. Choi, J. H. Kim and Y. S. Kang, *Macromolecules*, **34**, 9087 (2001).
26. J. Brandrup, E. H. Immergut and E. A. Grulke, 4th Ed., Polymer Handbook, John Wiley, New York (1999).
27. A. Shakoor and T. Z. Rizvi, *J. Raman Spectrosc*., **41**, 237 (2010).
28. A. Sluszny, M. S. Silverstein, N. Narkis and M. Narkis, *J. Appl. Polym. Sci*., **81**, 1429 (2001).